JGR Space Physics

RESEARCH ARTICLE
10.1029/2019JA027122

Poststorm Thermospheric NO Overcooling?

Andrey V. Mikhailov[1,2] and Loredana Perrone[2]

[1]Pushkov Institute of Terrestrial Magnetism, Ionosphere and Radio Wave Propagation, Troitsk, Russia, [2]Istituto Nazionale di Geofisica e Vulcanologia, Rome, Italy

Key Points:
- The existing F_2-layer storm mechanism is sufficient to explain the observed poststorm decrease in neutral gas density
- Storm-induced atomic oxygen variation is the controlling process
- There is no need to attract a new "poststorm NO overcooling" concept

Correspondence to:
L. Perrone,
loredana.perrone@ingv.it

Citation:
Mikhailov, A. V., & Perrone, L. (2020). Poststorm thermospheric NO overcooling?. *Journal of Geophysical Research: Space Physics*, *125*, e2019JA027122. https://doi.org/10.1029/2019JA027122

Received 2 JUL 2019
Accepted 23 DEC 2019
Accepted article online 31 DEC 2019

Abstract A mechanism of the neutral gas density decrease at middle latitudes during the recovery storm phase is discussed. The recently proposed method to retrieve thermospheric parameters from ionospheric observations is used for the analysis of equinoctial, summer, and winter severe magnetic storms. CHAllenging Minisatellite Payload and Swarm neutral gas density observations are used for a comparison. It is shown that storm-induced atomic oxygen variation is the controlling process. Well-known F_2-layer storm morphology and the poststorm decrease of neutral gas density reflect the same storm-induced variations of atomic oxygen abundance in the upper atmosphere. There is no need to attract a new "poststorm NO overcooling" concept to explain the decrease of neutral gas density.

The simplest explanation is best

(Occam's Razor)

1. Introduction

The analysis by Lei et al. (2012) of CHAllenging Minisatellite Payload (CHAMP) and Gravity field and steady state Ocean Circulation Explorer (GRACE) neutral gas density (ρ) variations along with NO cooling rates measured by Thermosphere Ionosphere Mesosphere Energetics and Dynamics/Sounding of the Atmosphere using Broadband Emission Radiometry for the October 2003 storm period has shown that the poststorm ρ values during the recovery storm phase were lower than the prestorm ones. Compared with the prestorm values, the maximum depletion in the CHAMP densities after the storm was about (16–23)% at 390 km, and the estimated with the MSISE00 model (Picone et al., 2002) decrease in thermospheric temperature on the dayside was as large as 110 K. The phenomenon was called "NO overcooling." That was one randomly chosen storm period but this has turned out to be sufficient to propose a new concept and to support it by TIEGCM model simulations (Chen & Lei, 2018) using a required temperature-dependent reaction rate of Duff et al. (2003). Later Zhang et al. (2019) have reanalyzed this effect considering both strongly disturbed and quiet time periods. They have shown that the effect may not take place for severe storms; on the other hand, they have stressed that a decrease in neutral density may be related with corresponding variations in solar EUV flux and a selection of the prestorm reference level. They have found that NO radiative cooling "may have very little to do with the density decrease." Their main conclusion is "thermospheric density decrease is likely caused by a combination of enhanced NO radiative cooling, reduced auroral energy input (HP and Joule heating), and reduced solar EUV flux." Such conclusion just indicates that the actual mechanism has not been revealed.

Neutral gas density at F_2 region heights is mainly specified by atomic oxygen concentration and exospheric temperature. Both parameters strongly change in the course of a storm and the mechanism of these changes is well-established (Duncan, 1969; Field et al., 1998; Forbes et al., 1996; Fuller-Rowell et al., 1994; Prölss, 1995; Rishbeth, 1998; Rishbeth et al., 1987; Rishbeth & Muller-Wodarg, 1999; Skoblin & Förster, 1993). Disturbed neutral composition with a decreased atomic oxygen concentration formed in the auroral zone is moved to middle latitudes by thermospheric winds resulted from the competition between solar-driven (background) and storm-induced circulations. The bulge of disturbed neutral composition with a decreased atomic oxygen concentration is pushed around by winds and may move back and forth in latitude (Prölss, 1995). Such effect was confirmed by the storm simulations (Fuller-Rowell et al., 1994) as well as by ESRO-4 data analysis (Skoblin & Förster, 1993). The bulge with disturbed neutral composition overlaps middle latitudes in the night and is shifted back to higher latitudes during daytime hours. This process may last for some days during a severe geomagnetic storm including the recovery storm phase.

The pattern strongly depends on season. In summer the $[O]/[N_2]$ disturbance zone may extend all the way from the polar to the low latitudes while in winter it is only restricted to high latitudes (Prölss, 1980; Prölss & von Zahn, 1977). The effect is due to the interaction of the seasonal (solar-driven) and storm-induced thermospheric circulations (Duncan, 1969; Field et al., 1998; Forbes et al., 1996; Fuller-Rowell et al., 1994).

A direct indication for the presence of a disturbed neutral composition at a given location is a decreased f_oF_2 compared to the quiet time or monthly median level. Therefore, if during the recovery storm phase a negative daytime F_2-layer storm effect takes place at middle latitudes one may expect a decreased neutral gas density at F_2-layer heights due to low atomic oxygen concentration. Such a decrease of neutral gas density may be not accompanied by a decrease in neutral temperature contrary to the NO overcooling concept by Lei et al. (2012).

The morphology of F_2-layer storms which reflects the state of disturbed thermosphere and the pattern of neutral winds is rather complicated and depends on the storm intensity, season, local time, latitude, and longitude of a place. For this reason a decrease in neutral gas density may not take place even after a strong geomagnetic storm as Zhang et al. (2019) have revealed for the 19–23 November 2003 storm event. In winter due to strong poleward thermospheric wind during daytime hours the disturbed neutral composition is restricted to high latitudes (Prölss, 1995; Prölss & von Zahn, 1977) and the negative storm phase (always related to low atomic oxygen concentration) will not appear at middle latitudes at least during daytime hours.

Zhang et al. (2019) have also given an example of a nonstorm event on 15–24 April 2013 when neutral gas density has manifested a pronounced decrease related to corresponding decrease in solar EUV. There is a class of F_2-layer perturbations occurring under quiet geomagnetic conditions, so called Q disturbances (Mikhailov et al., 2004, 2007). They may be both negative and positive. The formation mechanism of such disturbances is related to atomic oxygen concentration, solar EUV, and thermospheric wind variations. Therefore, one may expect a decrease (increase) of neutral gas density during such events as well.

In this paper using recently developed method by Perrone and Mikhailov (2018) to extract thermospheric parameters from daytime ionospheric observations we will analyze periods of strong geomagnetic storms resulting and nonresulting in neutral gas density decrease during the recovery storm phase. CHAMP and Swarm neutral gas density observations will be used in our analysis. The method by Perrone and Mikhailov (2018) has been modified to consider this particular problem by introducing the observed neutral gas density into the list of fitted parameters. The paper is aimed to demonstrate that a decrease of neutral gas density during the recovery storm phase can be explained within the framework of the well-known F_2-layer storm mechanism.

2. Method and Results

Our recently proposed method (Perrone & Mikhailov, 2018) can be successfully used to an analysis of neutral gas density variations during the recovery phase of strong geomagnetic storms and to answer the questions which Zhang et al. (2019) have formulated in relation with the NO overcooling concept. The method uses routinely observed (Reinisch et al., 2004) near-noontime f_oF_2 and plasma frequency f_o at 180 km from Global Ionosphere Radio Observatory (GIRO) database as the input information to retrieve neutral densities (O, O_2, N_2), exospheric temperature Tex, and vertical plasma drift W mainly related with thermospheric winds at middle latitudes. Formally the list of inferred parameters is sufficient for an analysis of neutral gas density variations at the location of ionospheric stations during geomagnetic storms. However, to attach the solution to the observed neutral gas density (ρ) the latter was added to the list of fitted parameters specially to consider the problem in question. To do this available CHAMP and Swarm neutral gas density observations in the daytime European sector were reduced to the location of ionosonde and 12 LT using the MSISE00 thermospheric model and the following expression:

$$\rho_{station} = \rho_{satellite} \frac{MSISE00_{station}}{MSISE00_{satellite}}$$

We have used three ρ observations from an orbit with the latitudes close to the latitude of ionosonde station and then found the mean of three reduced ρ values to use it in our analysis. Normally such three reduced ρ

Table 1
Relative Mean Deviation (in %) of Neutral Gas Density Reduction Using the MSISE00 Model and the Distance (in km) Between Two Analyzed Points in Latitudinal (lat) and Longitudinal (lon) Directions for the Storm Periods Analyzed in the Paper

Date	26/03/2015		20/03/2015		27/10/2003		01/11/2003		21/07/2004		28/07/2004		19/11/2003		24/11/2003	
Direct	lat	lon	lat	lon	lat	lon	lat	lon	lat	lon	lat	lon	Lat	lon	lat	lon
δ (%)	1.2	3.8	4.1	7.8	3.6	3.0	6.2	2.5	1.3	10.7	3.6	6.0	2.3	4.7	1.7	9.7
d (km)	1055	1699	1266	1647	1046	1715	1300	1619	1086	1682	1401	1695	1370	1710	1337	1712

values are very close to each other. The retrieved neutral gas density in our method $\rho = m_1[O] + m_2[O_2] + m_3[N_2]$ does not include the contribution of [He] and [N]; therefore, the observed neutral gas densities were corrected using MSISE-00. Depending on conditions this correction may be of (2–6)%. It should be noted that O, O_2, and N_2 concentrations are retrieved at heights $\leq h_mF_2$ and then they are recalculated to the height of ρ observation using the MSIS model temperature profile Tn(h) (Bates, 1959) normalized by the retrieved Tex value. During this reduction the height of ρ observation was kept unchanged not to introduce an additional uncertainty related to unknown MSISE00 neutral temperature Tex for the particular day in question. It should be stressed that during the reduction process we use relative (spatial and temporal) MSISE00 variations of thermospheric parameters that is the internal structure of the model. Our recent analysis of thermospheric parameter longitudinal variations (Mikhailov & Perrone, 2019, Table 2) has manifested a good coincidence between the retrieved and MSISE00 relative variations. As this reduction process raises questions we have undertaken an additional analysis. Normally there is always an orbit with neutral gas density observations not farther than ~10° in longitude from the ionosonde location. We selected two points along the orbit separated by ~10° in latitude and reduced the observed ρ to the other point using MSISE00. Then we compared the reduced ρ to the observed one in the second point to estimate the accuracy of the reduction procedure. The same procedure was applied for points at two neighboring orbits which are separated by ~22° in longitude and ~2 hr in UT. It should be stressed that this distance between neighboring orbits is by 2 times larger than a normal reduction distance of ~10° in longitude used in our method. We have analyzed four storm periods (see later) and for each we selected the reference (prestorm) day and the day belonging to the recovery storm phase. The results are given in Table 1 for relative deviations δ (in %) and the distance *d* (in km) between the compared points: average $\delta = 3.00 \pm 1.71\%$ in the latitudinal direction and $\delta = 6.02 \pm 3.09\%$ in the longitudinal direction. Keeping in mind that in reality the distance between the ionosonde and the nearest satellite orbit is less than ~10° in longitude we may accept that the inaccuracy of neutral density reduction from an orbit to the ionosonde location is (3–4)%. Therefore, there are no reasons not to rely on MSISE00 relative variations used in the reduction procedure.

We will consider geomagnetic storms during two equinoctial and summer periods when according to F_2-layer storm mechnism a decrease in neutral gas density should take place during the recovery storm phase, then we will analyze a winter storm when this effect should be absent at middle latitudes.

2.1. Intense Equinox Storm on 17–20 March 2015

The so-called St. Patrick Day storm on 17–20 March 2015 during the vernal equinox was a severe isolated storm with a quiet reference prestorm day on 16 March. Therefore, this period is an excellent case for our analysis. During some prestorm days geomagnetic activity was at a low level and solar activity manifested small variations (Figure 1). Along with $F_{10.7}$ and *AE* indices we have added to Figure 1 the total solar EUV (100–1,200) Å flux (Woods et al., 2018) to demonstrate the absence of any peculiarities with the ionizing radiation during the analyzed period.

Our analysis is based on ionospheric observations. For this reason let us consider f_oF_2 variations at the two European ionosonde stations Juliusruh (54.6°N, 13.4°E) and Rome (41.9°N, 12.5°E) where ionograms are scaled manually (Figure 2). These two stations will be also used in further analyses.

March 16 was a quite day with f_oF_2 close to monthly median value and it may be taken as a reference one. It should be stressed that in our analyses we use model f_oF_2 monthly medians specially produced for each

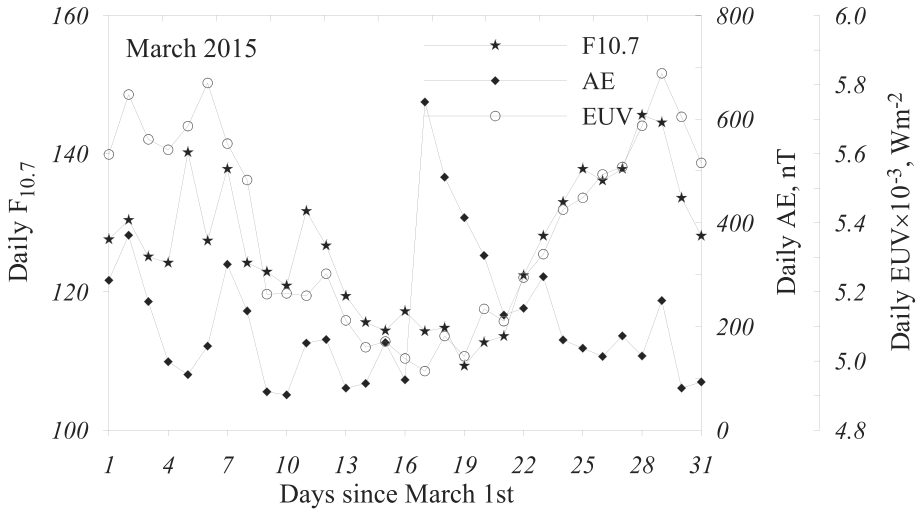

Figure 1. Daily $F_{10.7}$, *AE* indices, and solar EUV (100–1,200) Å variations in March 2015.

ionospheric station for 12 months and (00–23) UT moments using all available monthly median f_oF_2 observations and IPS T-index (Caruana, 1990; Turner, 1968) as an indicator of the solar activity level.

The first splash of auroral activity at (06–09) UT on 17 March with *AE* index increase up to 778 nT produced a well-pronounced positive storm phase in f_oF_2 at middle latitude related with the TAD passage. The positive phase was immediately followed by a negative one at Juliusruh clearly indicating the arrival of disturbed

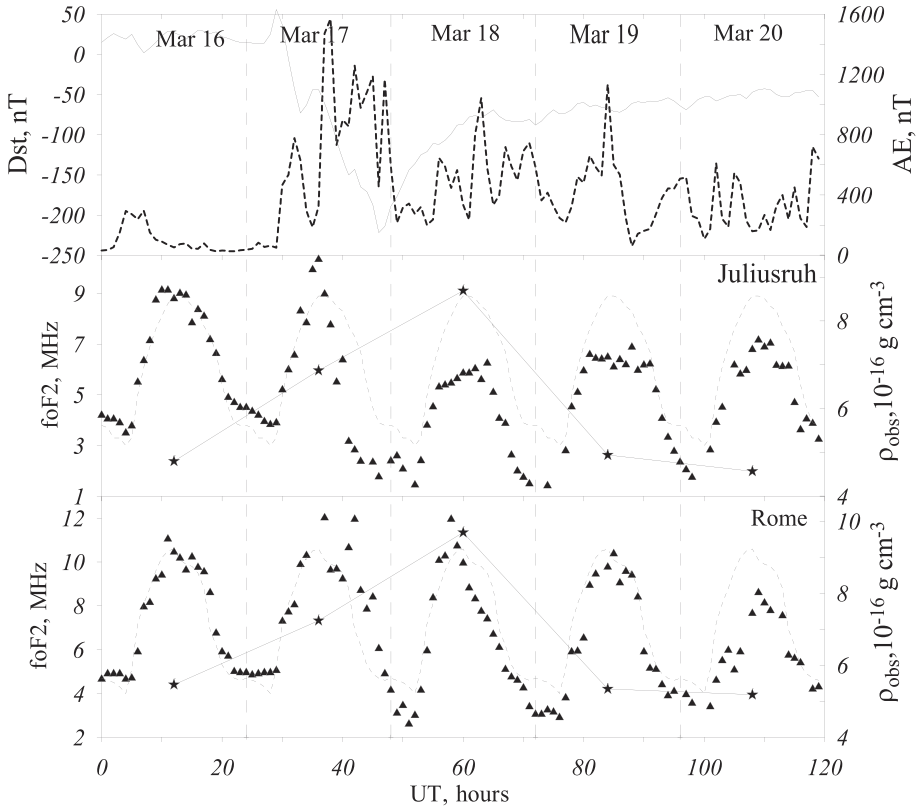

Figure 2. Observed hourly and monthly median (dashes) f_oF_2 variations at Juliusruh and Rome for the 16–20 March 2015 geomagnetic storm. Observed hourly *Dst* (solid line) and *AE* (dashes) indices are shown in the top panel. Asterisks = reduced to Juliusruh (at 516.5 km) and Rome (at 513.9 km) Swarm-B neutral gas densities.

Table 2
Retrieved Tex, [O], and ρ for Juliusruh at 516.5 km for the March 2015 Geomagnetic Storm

Parameter	16 March	17 March	18 March	19 March	20 March
ρ_{obs} (10^{-16} g cm^{-3})	4.80	6.87	8.69	4.94	4.57
ρ_{MSISE} (10^{-16} g cm^{-3})	*5.59*	*6.89*	*7.08*	*6.74*	*5.90*
Tex (K)	990	1115	1247	1075	1082
[O] (10^7 cm^{-3})	1.77	2.45	2.86	1.77	1.62
Daily $F_{10.7}$	117.2	114.3	114.8	109.3	112.7
Daily *Ap* (nT)	12	108	47	26	22

Note. Swarm neutral gas densities reduced to Juliusruh (12 LT) as well as MSISE00 (italic) values are given for a comparison. Daily $F_{10.7}$ and *Ap* indices are given in the bottom. Shadow indicates the reference day.

neutral composition. Therefore, that was a classic two-phase F_2-layer storm normally occurring when a storm commencement takes place during daytime hours (Mikhailov et al., 2012).

Negative f_oF_2 deviations at Juliusruh took place during three days (18–20 March) both in nighttime and daytime hours indicating the presence of disturbed neutral composition. Rome located farther from the auroral zone manifested negative deviations mainly during nighttime hours when the thermospheric circulation was equatorward. However, as the auroral activity was elevated during the recovery storm phase the ionospheric negative storm phase appeared at Rome on 20 March during daytime hours as well (Figure 2).

The reduced to ionosonde locations Swarm neutral gas densities indicate some (~5%) decrease on 20 March with respect to the prestorm level on 16 March at both stations (Figure 2 and Tables 2 and 3) looking like a confirmation for the NO overcooling concept. This difference may be slightly increased if neutral gas density (ρ) observed on 20 March under $Ap = 22$ to reduce to $Ap = 12$ on 16 March. But we have not done this reduction keeping in mind that the difference in *Ap* is not large and $F_{10.\ 7}$ were very close for the two days in question (Table 2). It should be mentioned that the accuracy of Swarm neutral gas density observations has not been officially declared yet. Everywhere (Tables 2–9) the observed neutral gas densities after the reduction to the location of ionosonde stations (see earlier) are given in a comparison to the MSISE00 (Picone et al., 2002) model. It is seen that MSISE00 does not reproduce the poststorm decrease in neutral gas density (Tables 2 and 3).

Neutral gas density is mainly presented by atomic oxygen at heights in question. This is seen from MSISE00 model calculations for the Rome location at 515-km height on 20 March 2015 (12 LT): $[O] = 2.37 \times 10^7$ cm^{-3}, $[N_2] = 3.67 \times 10^5$ cm^{-3}, $[O_2] = 5.39 \times 10^3$ cm^{-3}. Tables 2 and 3 indicate a 9% decrease in the retrieved atomic oxygen on 20 March compared to 16 March despite larger Tex during the recovery storm phase. The difference in Tex means that the total (column) decrease in the atomic oxygen abundance is essential during the recovery storm phase. This result agrees with the present day understanding of the F_2-layer storm mechanism mentioned earlier. Thus, the analyzed equinoctial storm event does demonstrate a decrease in neutral gas density during the recovery storm phase compared to the prestorm reference day but this decrease is due to a decrease in atomic oxygen abundance in the upper atmosphere. Along with this (contrary to the poststorm NO overcooling concept) neutral temperature Tex is larger (Tables 2 and 3) compared to the prestorm reference day and this is due to larger *Ap* during the recovery storm phase. It should be noted that MSISE00 also gives larger Tex on 20 March compared to 16 March.

A partial solar eclipse took place on 20 March with a 78% coverage of the Sun at Juliusruh and a 54% coverage at Rome. The eclipse with duration of 2 hr and 18 min has completely ended by noontime at both locations. Therefore, some decrease in electron density may be attributed to a decrease in solar EUV before noontime; however, this cannot change the main conclusion on the storm-induced decrease in the atomic oxygen abundance which takes place during other storm events considered in the paper.

2.2. Intense Equinoctial Storm on 28–31 October 2003

This storm was considered by Lei et al. (2012), Chen and Lei (2018), and Zhang et al. (2019) and their analyses have resulted in the "poststorm NO overcooling" concept. An interesting peculiarity of that period was a steep increase of solar activity after 18 October (Figure 3). Under monthly median $F_{10.7}$~150 with noontime

Table 3
Same as Table 2 but for Rome (513.9 km)

Parameter	16 March	17 March	18 March	19 March	20 March
ρ_{obs} (10^{-16} g cm^{-3})	5.46	7.24	9.69	5.34	5.18
ρ_{MSISE} (10^{-16} g cm^{-3})	*6.23*	*7.62*	*7.92*	*7.52*	*6.56*
Tex (K)	998	1110	1159	1059	1070
[O] (10^7 cm^{-3})	2.03	2.59	3.42	1.92	1.86

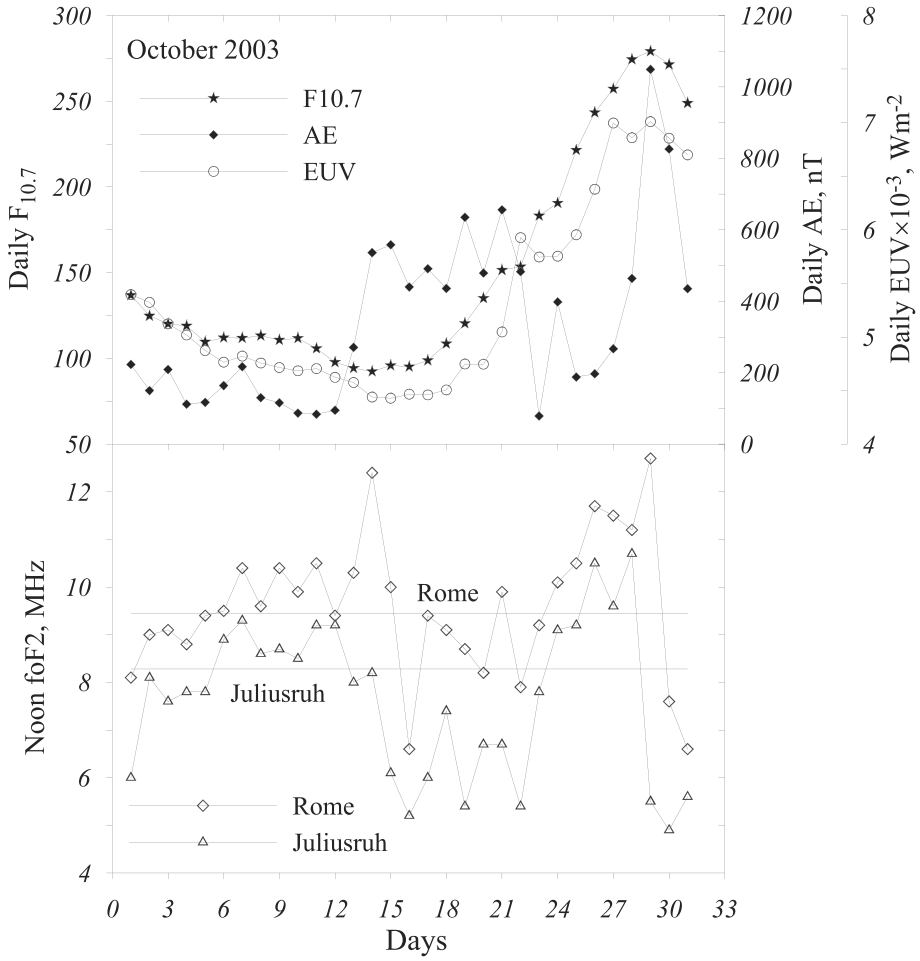

Figure 3. (top panel) Daily $F_{10.7}$, *AE* indices, and solar EUV (100–1,200) Å variations. (bottom panel) Noontime f_oF_2 variations at Rome and Juliusruh in October 2003. Straight lines = noontime monthly median f_oF_2 values at the two stations.

median f_oF_2~(8–9) MHz at Juliusruh and Rome solar radio flux has increased up to $F_{10.7}$~280 on 29 October resulting in f_oF_2~(11–13) MHz. Formally from ionospheric point of view all f_oF_2 values during 24–29 October at Rome and 24–28 October at Juliusruh were positively disturbed followed by negative f_oF_2 deviations.

Following strongly varying $F_{10.7}$ the total solar EUV (100–1,200) Å flux was also very large after 13 October (Figure 3). Despite the increasing intensity of solar EUV f_oF_2 fell down below median level after 15 October. This was due to storm effect related to elevated auroral activity with *AE*~500 nT (Figure 3; right *y* axis)

Table 4
Retrieved Tex, [O], and [N_2] at Juliusruh (397.7 km) for the October 2003 Geomagnetic Storm

Parameter	26 October	27 October	28 October	29 October	30 October	31 October	01 November
ρ_{obs} (10^{-15} g cm^{-3})	5.05	6.39	8.96	10.16	6.66	7.72	5.19
ρ_{MSISE} (10^{-15} g cm^{-3})	*7.14*	*7.94*	*8.81*	*12.74*	*11.59*	*12.36*	*8.80*
Tex (K)	1114	1202	1328	1579	1447	1455	1231
[O] (10^8 cm^{-3})	1.71	2.09	2.66	1.89	1.14	1.56	1.56
[N_2] (10^7 cm^{-3})	1.07	1.74	3.78	10.37	7.41	7.36	2.18
Daily $F_{10.7}$	243.4	257.2	274.4	279.1	271.4	248.9	210.4
Daily *Ap* (nT)	10	11	25	204	191	116	26

Note. CHAMP/STAR and reduced to Juliusruh (12 LT) as well as MSISE00 (italic) neutral gas densities are given for a comparison. Daily $F_{10.7}$ and *Ap* indices are given in the bottom. Shadow indicates the reference day, 27 October.

inevitably resulting in neutral composition changes. This F_2-layer storm mechanism is mentioned repeatedly in the paper; therefore, it is appropriate to give the expression relating daytime midlatitude N_mF_2 to the main aeronomic parameters (Ivanov-Kholodny & Mikhailov, 1986; Mikhailov et al., 1995)

$$N_mF2 \propto \frac{J_0[0]^{2/3}}{T_n{}^{5/6}} \left(\frac{0}{N_2}\right)^{2/3} \quad (1)$$

where J_o is the ionization efficiency which is proportional to the total incident ionizing solar EUV flux, T_n is the neutral temperature, [O] is the atomic oxygen, and [N_2] is the molecular nitrogen concentrations at a fixed height in the F_2 region (say 300 km). Expression (1) shows that N_mF_2 depends not only on the O/N_2 ratio but also on the absolute concentration of atomic oxygen as well. For this reason [O] is a crucial parameter both for N_mF_2 and neutral gas density (see earlier). Therefore, a decrease in f_oF_2 after 15 October reflects changes in neutral composition which overpower the increase in solar EUV.

October 27 used by Lei et al. (2012) as a reference (prestorm) day in fact was a disturbed one with splashes of *AE* index up to 490 nT indicating a disturbed thermosphere. On 30–31 October during the recovery storm phase geomagnetic activity was still high with daily $AE > 400$ nT (Figure 3 and Table 4) and daily $Ap =$ 191 and 116, correspondingly. Therefore, the whole recovery period was strongly contaminated with geomagnetic storm effects. Nevertheless, for a comparison with the results by Lei et al. (2012) we will consider this storm period as it was used to propose the "NO overcooling concept."

CHAMP/STAR daytime neutral gas density observations are available for this period in the daytime European sector. Observed neutral gas densities on 26 October to 01 November were reduced to the locations of Rome and Juliusruh, 12 LT (as this was mentioned earlier).

Our analysis is based on ionospheric observations; therefore, f_oF_2 variations during this storm period are given in Figure 4. The prestorm reference day 27 October was positively disturbed mainly due to large $F_{10.7} = 257.2$ (and correspondingly large ionizing solar EUV flux; Figure 3). On 29 October solar activity remained at a very high level ($F_{10.7} = 279.1$) and auroral activity was also very strong with splashes of *AE* index up to 2,000 nT (Figure 4). The latter has resulted in a negative storm phase at Juliusruh but not at Rome as the bulge of disturbed neutral composition has reached the Rome location only in the night (see a negative storm phase during the 29–30 October night). Both days of 30–31 October were negatively disturbed at the two stations. Daytime f_oF_2 are below median values on 01 November and neutral gas density remained at a low level (Figure 4 and Tables 4 and 5) looking like a confirmation of the NO overcooling concept.

Our method (Perrone & Mikhailov, 2018) including the observed neutral gas density as a fitted parameter was applied to ionospheric observations at the two stations and the inferred aeronomic parameters are given in Tables 4 and 5. MSISE00 fails to reproduce ρ variations (Tables 4 and 5) for such supper storm conditions and this is explainable.

Tables 4 and 5 show that the observed neutral gas density on 30–31 October (the recovery storm phase) is not less compared to the reference day of 27 October, but Tex was much larger on 30–31 October due to large *Ap* and $F_{10.7}$ indices compared to 27 October. Any strict reduction of thermospheric parameters obtained for 30–31 October to conditions of the reference day is impossible but a formal change of exospheric temperature for Tex of the reference day in the MSISE00 model gives a decrease in neutral gas density by a factor of 2 at heights in question. November 01 (also belonging to the recovery storm phase) with Tex which is much closer to Tex of the reference day manifests a 19% decrease in ρ at Juliusruh and a 24% decrease at Rome.

Thus, the recovery storm phase (01 November) does demonstrate a decrease in neutral gas density compared to the prestorm reference day but this decrease is totally due to a storm-induced decrease in the atomic oxygen abundance (the main contributor to ρ at heights in question; see also [N_2] in Tables 4 and 5). The decrease of [O] is strong and is seen even under large Tex taking place on 30–31 October (Tables 4 and 5). This result contradicts the NO overcooling concept which relates the observed decrease in neutral gas density with a poststorm cooling of the upper atmosphere. Under extremely disturbed geomagnetic conditions with daily $Ap =$ 191 and 116 nT on 30–31 October compared to $Ap = 11$ nT and $F_{10.7}$ which are also larger than on the reference day (Table 4) neutral temperature cannot be lower on 30–31 October than on 27

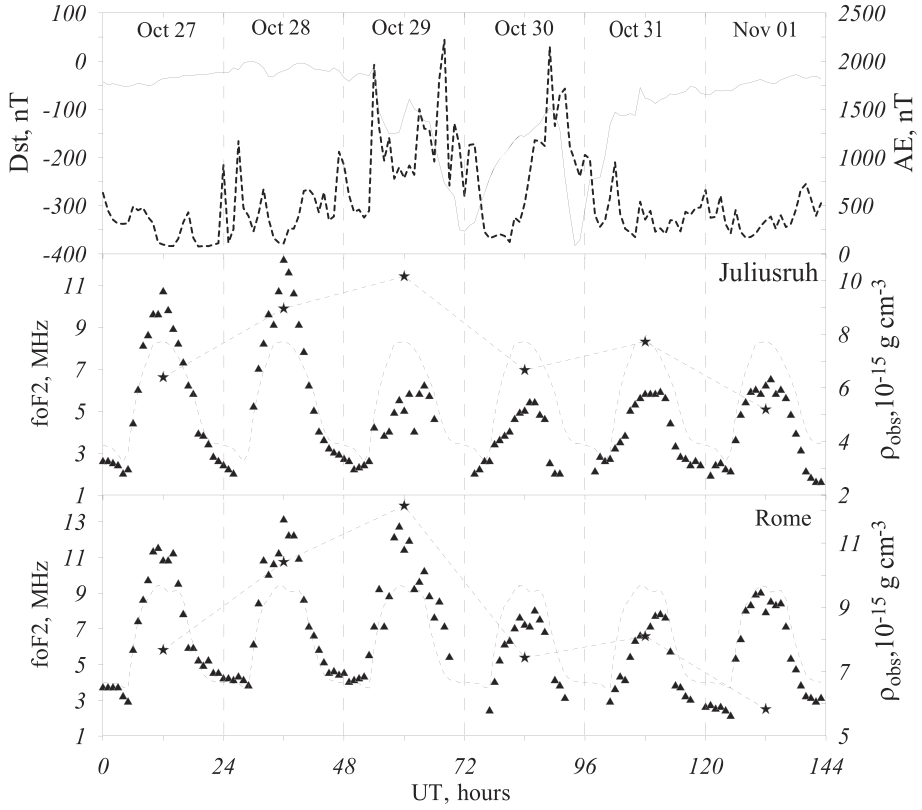

Figure 4. Observed hourly and monthly median (dashes) f_oF_2 variations at Juliusruh and Rome for the 27–31 October 2003 geomagnetic storm. Observed hourly *Dst* (solid line) and *AE* indices are shown in the top panel. Asterisks = reduced to Rome (at 395.5 km) and Juliusruh (at 397.7 km) CHAMP/STAR neutral gas densities.

October. The reliability of this result is based on the coincidence of the observed and retrieved neutral gas densities as well as on f_oF_2, both directly depending on exospheric temperature and the concentration of atomic oxygen. Moreover, any empirical thermospheric model will predict larger Tex for the conditions of 30–31 October compared to 27 October contrary to the NO overcooling concept.

2.3. Intense Summer Storm on 22–30 July 2004

According to the present day understanding of the thermosphere-ionosphere storm mechanism a storm-induced decrease of the thermospheric neutral gas density should take place in summer season as well. A strong long-lasting storm during the 22–30 July 2004 period has been selected to demonstrate this effect. That was an isolated storm consisting of three storm commencement and corresponding three splashes of auroral activity up to AE = 1,200–1,800 nT (Figures 5 and 6). July 21 with daily Ap = 4 nT may be used as an excellent reference prestorm day while 28–30 July may be considered as the days belonging to the recovery storm phase (Figure 6). Figure 5 and Table 6 show that solar activity manifested a strong decrease from

Table 5
Same as Table 4 but for Rome at 395.5 km

Parameter	26 October	27 October	28 October	29 October	30 October	31 October	01 November
ρ_{obs} (10^{-15} g cm^{-3})	5.89	7.67	10.41	12.16	7.43	8.10	5.83
ρ_{MSISE} (10^{-15} g cm^{-3})	*7.91*	*8.77*	*9.73*	*13.96*	*13.10*	*13.94*	*9.92*
Tex (K)	1141	1224	1337	1449	1396	1466	1150
[O] (10^8 cm^{-3})	1.99	2.53	3.04	3.29	1.66	1.78	1.92
[N_2] (10^7 cm^{-3})	1.24	2.00	4.04	7.04	6.18	7.02	1.57

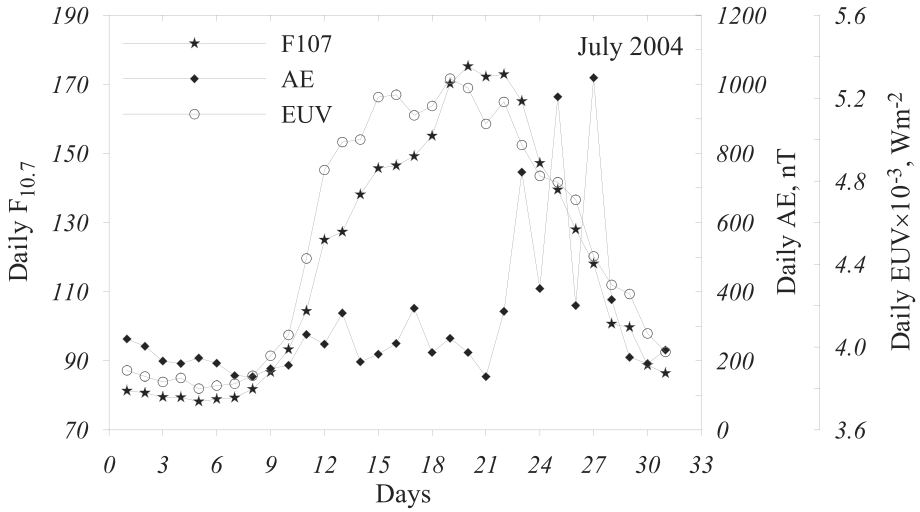

Figure 5. Daily $F_{10.7}$, *AE* indices, and solar EUV (100–1,200) Å variations in July 2004.

$F_{10.7}$ = 172.2 on 21 July down to $F_{10.7}$ = 88.7 on 30 July. This means that a large part of neutral gas density decrease during the recovery storm phase was due to this decrease of solar activity and this should be taken into account in our analysis.

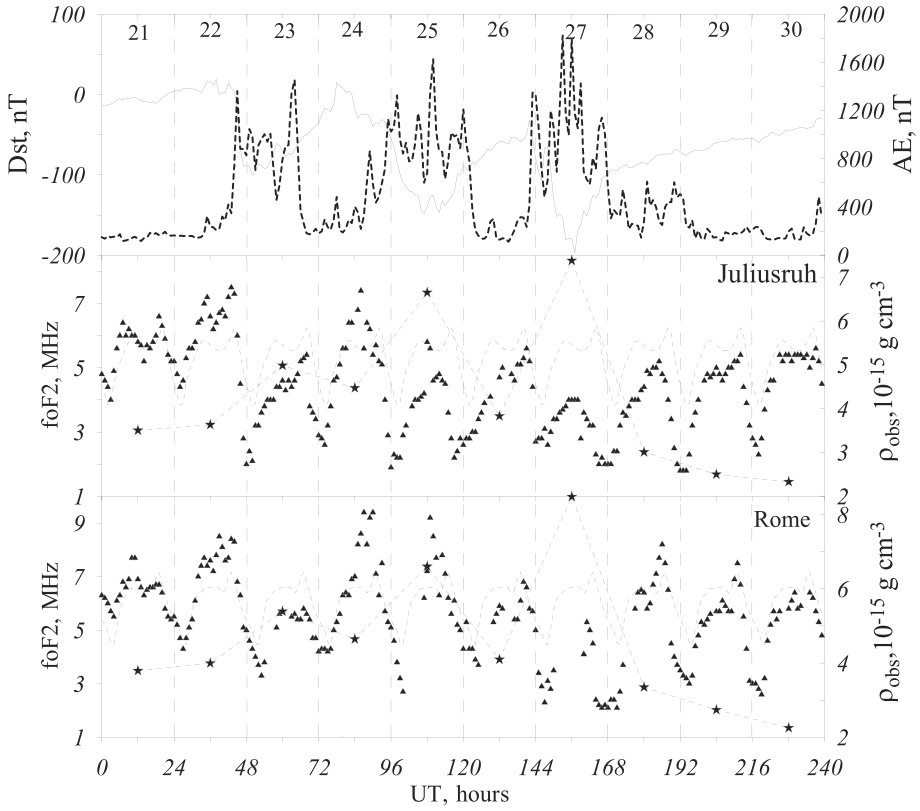

Figure 6. Observed hourly and monthly median (dashes) f_oF_2 variations at Juliusruh and Rome for the 22–30 July 2004 geomagnetic storm. Observed hourly *Dst* (solid line) and *AE* indices are shown in the top panel. Asterisks = reduced to Juliusruh (at 383.0 km) and Rome (at 380.5 km) CHAMP/STAR neutral gas densities.

Table 6
Retrieved Tex, [O], [N_2], and Vnx at Juliusruh (383.0 km) for the July 2004 Geomagnetic Storm

Parameter	21 July	22 July	23 July	24 July	25 July	26 July	27 July	28 July	29 July	30 July
ρ_{obs} (10^{-15} g cm^{-3})	3.50	3.63	4.98	4.47	6.65	3.83	7.38	3.01	2.50	2.33
ρ_{MSISE} (10^{-15} g cm^{-3})	*4.46*	*4.45*	*5.79*	*5.01*	*6.29*	*4.68*	*6.47*	*4.08*	*3.09*	*2.89*
Tex (K)	1097	1074	1298	1120	1314	1186	1337	1099	980	958
[O] (10^7 cm^{-3})	9.70	11.01	8.19	12.85	11.23	7.40	11.47	7.09	7.27	7.15
[N_2] (10^7 cm^{-3})	1.96	1.49	5.86	2.23	7.56	4.05	8.82	2.37	1.20	0.92
Vnx (m s^{-1})	−38.9	−28.9	+91.0	−31.3	+90.6	+52.0	+90.5	−28.3	−29.8	−29.8
Daily $F_{10.7}$	172.2	172.9	165.1	147.2	131.5	128.0	118.1	100.7	99.7	88.7
Daily *Ap* (nT)	4	31	52	37	154	47	186	15	6	7

Note. CHAMP/STAR and reduced to Juliusruh (12 LT) as well as MSISE00 (italic) neutral gas densities are given for a comparison. Daily $F_{10.7}$ and *Ap* indices are given in the bottom. Shadow indicates the reference day, 21 July.

Unfortunately DPS-4 Ne(h) observations are absent for some days during the period in question both at Juliusruh and Rome and available manually scaled f_oF_1 data were requested directly from the ionosondes. Our method (Perrone & Mikhailov, 2018) has a version using f_oF_1 instead of plasma frequency at 180 km, f_{o180}, and this version may be used in summer when f_oF_1 observations are available. CHAMP/STAR neutral gas density observations were used in the retrieval process as this was mentioned earlier.

Figure 6 shows that daytime f_oF_2 on the reference day are close to monthly median values both at Juliusruh and Rome while days during the recovery storm phase mainly demonstrate negative deviations indicating a disturbed neutral composition. Nighttime f_oF_2 values fell down to ~2 MHz telling us about strongly perturbed thermosphere.

Observed in a comparison to MSISE00 neutral gas densities as well as inferred Tex, [O], and [N_2] are given in Tables 6 and 7 for Juliusruh and Rome stations. Although ρ values during the recovery storm phase (28–30 July) are lower than on 21 July this difference is mainly due to lower $F_{10.7}$ on 28–30 July (Table 6). Keeping in mind that MSISE00 is driven by $F_{10.7}$ and *Ap* indices we may compare the inferred to model ρ_{day}/ρ_{ref} ratios and to check if there an additional difference in ρ not related to $F_{10.7}$ and *Ap* index variations. The undertaken analysis of data in Tables 6 and 7 has shown that only 28 July manifests an additional ρ decrease of 5–7% while the decrease in ρ on 29–30 July is completely attributed to the decrease in solar activity. In fact 29–30 July were magnetically quiet days with $Ap = 6$ and 7 nT (Table 6). The effective meridional thermospheric wind Vnx = W/sinIcosI (I-magnetic inclination) is given in Table 6 for further comparison with winter storm results.

Therefore, the summer recovery storm phase similar earlier analyzed equinoctial storm cases manifest a decrease in neutral gas density with respect to the prestorm reference day and this decrease is due to the storm-induced decrease in the atomic oxygen abundance.

2.4. Intense Winter Storm on 20–24 November 2003

This was a severe winter storm analyzed by Zhang et al. (2019) which did not manifest any NO overcooling effect with a decrease in neutral density during the recovery storm phase and this has caused many questions left unanswered. The storm occurred at the rising phase of solar activity and the previous (09–18 November)

Table 7
Same as Table 6 but for Rome at 380.5 km

Parameter	21 July	22 July	23 July	24 July	25 July	26 July	27 July	28 July	29 July	30 July
ρ_{obs} (10^{-15} g cm^{-3})	3.79	3.99	5.39	4.64	6.60	4.09	8.48	3.35	2.74	2.25
ρ_{MSISE} (10^{-15} g cm^{-3})	*4.92*	*4.91*	*6.41*	*5.54*	*6.89*	*5.12*	*7.04*	*4.56*	*3.38*	*3.18*
Tex (K)	1036	1130	-	1158	1257	1197	-	1001	985	930
[O] (10^7 cm^{-3})	12.27	10.43	-	12.23	14.98	8.99	-	10.46	8.13	7.17
[N_2] (10^7 cm^{-3})	1.28	2.58	-	2.92	5.44	3.59	-	1.20	1.22	0.78

Note. Dashes = ionospheric observations are absent.

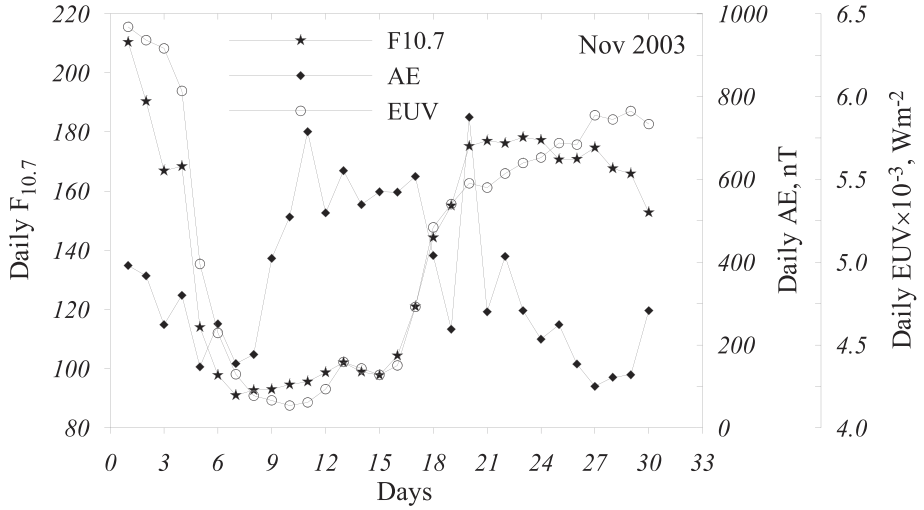

Figure 7. Daily $F_{10.7}$, *AE* indices, and solar EUV (100–1,200) Å variations in November 2003.

period was magnetically disturbed (Figure 7). However, keeping in mind the peculiarity of winter circulation with a strong poleward wind (see later) during daytime hours 19 November with $Ap = 12$ nT may be taken as a reference prestorm day, f_oF_2 variations were also close to monthly median (Figure 8) indicating undisturbed neutral composition.

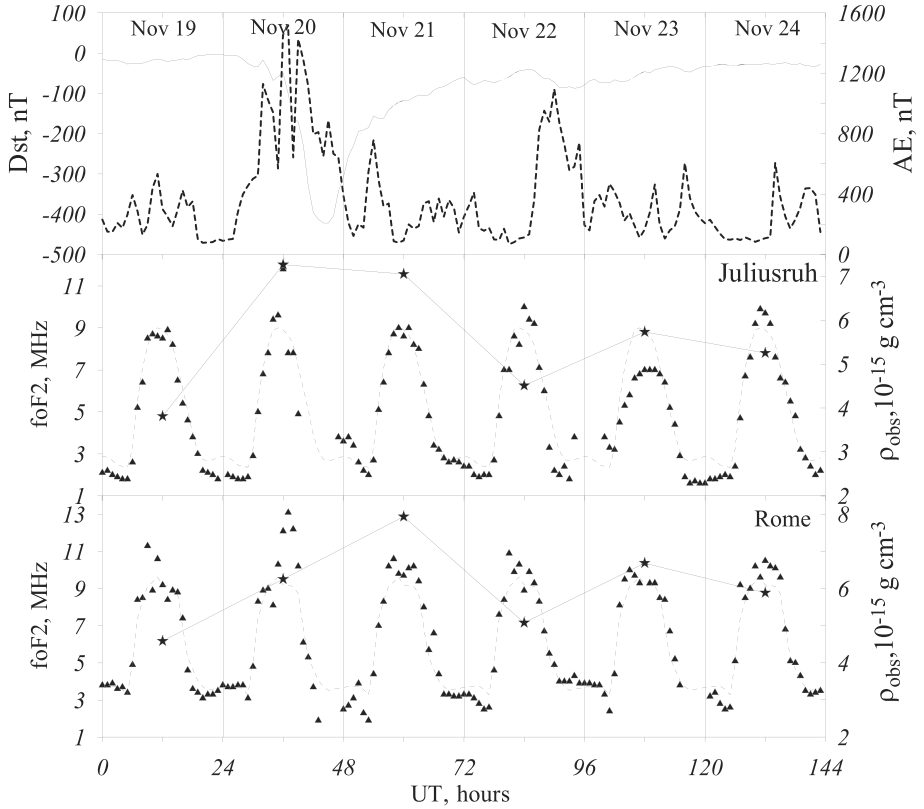

Figure 8. Observed hourly and monthly median (dashes) f_oF_2 variations at Juliusruh and Rome for the 20–24 November 2003 geomagnetic storm. Observed hourly *Dst* (solid line) and *AE* indices are shown in the top panel. Asterisks = reduced to Juliusruh (at 394.8 km) and Rome (at 392.0 km) CHAMP/STAR neutral gas densities.

Table 8
Retrieved Tex, [O], [N_2], and Vnx at Juliusruh at 394.8 km for the November 2003 Geomagnetic Storm

Parameter	19 November	20 November	21 November	22 November	23 November	24 November
ρ_{obs} (10^{-15} g cm^{-3})	3.81	7.26	7.05	4.51	5.73	5.25
ρ_{MSISE} (10^{-15} g cm^{-3})	*4.92*	*6.19*	*7.14*	*5.95*	*6.08*	*5.68*
Tex (K)	987	1203	1255	1043	1177	1054
[O] (10^8 cm^{-3})	1.34	2.13	2.03	1.55	1.82	1.82
[N_2] (10^7 cm^{-3})	0.56	3.34	3.45	0.82	1.90	0.85
Vnx (m s^{-1})	−65.6	+91.5	+60.8	−59.2	−63.2	−58.3
Daily $F_{10.7}$	155.1	175.2	177.0	176.2	178.2	177.3
Daily *Ap* (nT)	12	150	42	30	22	13

Note. CHAMP/STAR and reduced to Juliusruh (12 LT) as well as MSISE00 (italic) neutral gas densities are given for a comparison. Daily $F_{10.7}$ and *Ap* indices are given in the bottom. Shadow indicates the reference day, 19 November.

Despite strong auroral activity on 20 November with $AE > 1{,}400$ nT f_oF_2 show small variations being close to monthly median values or manifesting small positive deviations during daytime hours (Figure 8). Only 23 November demonstrates negative deviations at Juliusruh as the reaction to the 22 November evening splash of auroral activity. Nighttime equatorward circulation was able to transfer the disturbed neutral composition to latitudes of Juliusruh but not of Rome where f_oF_2 variations were close to median ones on 23 November (Figure 8).

Inferred Tex, [O], [N_2], and Vnx are given in Tables 8 and 9 for Juliusruh and Rome. Observed with CHAMP/STAR and reduced to the ionosonde location (12 LT) as well as MSISE00 (italic) neutral gas densities are given for a comparison. November 20–22 were disturbed days (see *AE* and *Ap* indices Figure 8 and Table 8) while 23 and 24 November were more quiet and may be analyzed as the days belonging to the recovery storm phase. Tables 8 and 9 show that the observed neutral gas densities were larger on these days compared to the reference day, 19 November. Partly this is due to larger $F_{10.7}$ and *Ap* (Table 8) and partly to storm-induced neutral composition. To separate these two contributions ρ_{day}/ρ_{ref} ratios may be analyzed (Table 10) using the observed and MSISE00 neutral gas densities from Tables 8 and 9. The MSISE00 model is driven by $F_{10.7}$ and *Ap* indices; therefore, the model ratios are the same at Juliusruh and Rome (Table 10) while the inferred ratios are different as they reflect the real pattern of the storm in question. The observed ρ_{day}/ρ_{ref} ratios are larger than model ones for 23 and 24 November indicating larger changes of atomic oxygen (the main contributor to neutral gas density at heights in question) than may be attributed to $F_{10.7}$ and *Ap* variations. Table 10 shows that the difference is around 50% telling us that half of the observed neutral gas density increase is due to storm-induced atomic oxygen variation.

The revealed variations of atomic oxygen may be explained in the framework of solar-driven and storm-induced thermospheric circulation interaction (e.g., Rishbeth, 1998, and references therein). The interaction of strong poleward wind (Tables 8 and 9) with oppositely directed storm-induced circulation results in downwelling increasing the atomic oxygen abundance. This increases neutral gas density—the situation we have on 23 and 24 November during the recovery storm phase.

Thus, the dependence of F_2-layer storm mechanism on season explains the absence of neutral gas density decrease during the winter recovery storm phase.

Table 9
Same as Table 8 but for Rome at 392.0 km

Parameter	19 November	20 November	21 November	22 November	23 November	24 November
ρ_{obs} (10^{-15} g cm^{-3})	4.59	6.25	7.93	5.08	6.69	5.88
ρ_{MSISE} (10^{-15} g cm^{-3})	*5.65*	*6.90*	*8.19*	*6.82*	*6.95*	*6.50*
Tex (K)	1014	1229	1290	1069	1118	1087
[O] (10^8 cm^{-3})	1.60	1.75	2.26	1.74	2.28	2.02
[N_2] (10^7 cm^{-3})	0.71	3.44	4.02	0.94	1.32	1.06
Vnx (m s^{-1})	−50.4	+64.7	+41.5	−48.4	−48.2	−48.0

Table 10
Observed and MSISE00 ρ_{day}/ρ_{ref} Ratios at Juliusruh and Rome

	Juliusruh		Rome	
Data	23/19 November	24/19 November	23/19 November	24/19 November
Observed	1.50	1.38	1.45	1.28
MSISE00	1.23	1.15	1.23	1.15

3. Discussion

Midlatitude daytime ionospheric F_2 layer is a good indicator for the state of the thermosphere both under quiet and disturbed conditions. Electron concentration N_mF_2 depends on the intensity of solar EUV radiation, neutral composition (O, O_2, N_2), temperature Tex, and on vertical plasma drift mainly related to thermospheric winds. Neutral gas density at a fixed height of a satellite also depends on (O, O_2, N_2) and temperature Tex. Therefore, fitting observed ρ, N_mF_2, and five values of electron concentration at F_1-region heights in accordance with our method (Perrone & Mikhailov, 2018) we obtain a complete and consistent set of the main aeronomic parameters necessary to analyze the problem of poststorm neutral gas density variations.

Undoubtedly, the effect of NO cooling exist in the upper atmosphere and it may be important for something but the poststorm decrease of neutral gas density (when it takes place) has a clear explanation based on well-known thermosphere-ionosphere storm mechanism proposed years ago and repeatedly confirmed both by observations and model simulations (Duncan, 1969; Field et al., 1998; Forbes et al., 1996; Fuller-Rowell et al., 1994; Prölss, 1995; Rishbeth, 1998; Rishbeth et al., 1987; Rishbeth & Muller-Wodarg, 1999; Skoblin & Förster, 1993). The idea of this mechanism has been outlined in the Introduction part but it would be useful to repeat here its main points for the discussion of obtained results. The thermosphere-ionosphere storm process starts with heating of the auroral zone due to Joule heating by magnetospheric electric fields and particle precipitations the latter being less important. The neutral temperature increase gives rise to upwelling resulting in the O/N_2 ratio decrease at *F*-layer heights. Elevated neutral gas pressure (due to the increased neutral gas temperature) changes the distribution of pressure gradients in the upper atmosphere and the global thermospheric circulation, correspondingly. During nighttime hours the equatorward solar-driven meridional wind coincides with the storm-induced one and the perturbed neutral composition with low O/N_2 is shifted equatorward producing negative F_2-layer disturbances even at low-latitude stations such as Rome (Figure 2). Negative F_2-layer disturbances mainly take place during early morning and for some prenoon hours while the daytime poleward solar-driven circulation does not shift the disturbed neutral composition back to higher latitudes. If a magnetic storm and auroral heating are strong enough the storm-induced equatorward circulation overpowers the solar-driven one and the disturbed neutral composition with low O/N_2 ratio occurs at middle latitudes during daytime hours as well (30–31 October at Rome). It should be reminded that disturbed neutral composition with low O/N_2 ratio corresponds to low neutral gas density as atomic oxygen is the main constituent at F_2-layer heights. Along with this neutral temperature Tex may be larger compared to the quiet reference day (see Tables 2 and 3). This depends on the level of geomagnetic activity during the recovery storm phase. It should be stressed that the St. Patrick storm case (Figure 2 and Tables 2 and 3) is more "clear" compared to the 28–31 October 2003 one analyzed by Lei et al. (2012), Chen and Lei (2018), and Zhang et al. (2019). During the St. Patrick storm solar activity was rather stable (Figure 1 and Table 2) unlike the 28–31 October 2003 period when $F_{10.7}$ manifested large variations and some poststorm effects were related to $F_{10.7}$ variations. The St. Patrick storm case may be considered as a classic one which clearly demonstrates the main features of the F_2-layer storm mechanism indicating a decrease of neutral gas density during the recovery storm phase on 20 March due to a decrease in the atomic oxygen abundance along with increased neutral temperature compared to the reference prestorm day (Tables 2 and 3).

The "NO overcooling" concept fails to explain the winter storm (Zhang et al., 2019). However, the observed neutral gas density variations have a simple explanation within the F_2-layer storm mechanism. In accordance with this mechanism in winter the disturbed neutral composition is restricted to high latitudes (Prölss, 1980; Prölss & von Zahn, 1977) while at middle latitudes one should expect an increase of atomic

oxygen abundance due to downwelling (Rishbeth, 1998). Contrary to the NO overcooling concept CHAMP observations indicate an increase of neutral gas density due to increase of the atomic oxygen abundance as our calculations show (Tables 8 and 9).

One should only wonder why the authors of the NO overcooling concept have not even mentioned the thermosphere-ionosphere storm mechanism as a possible explanation despite obvious contradictions with this concept listed by Zhang et al. (2019).

The term "overcooling" implies a decrease of thermospheric temperature with respect to the reference prestorm day. Assuming that observed changes of thermospheric mass density are purely attributable to changes in thermosphere temperature Lei et al. (2012) using MSISE00 have found a Tex decrease of 110 K on the dayside. However, normally auroral activity is kept elevated during the recovery storm phase (see earlier analyzed storm cases) and Tex just cannot be lower compared to a quiet time prestorm Tex value. All empirical thermospheric models based on observations tell this. The only plausible explanation is to attribute the observed neutral gas density decrease to a decrease in the atomic oxygen concentration (the main contributor to ρ at heights in question). This is predicted by F_2-layer storm mechanism and is confirmed by our calculations.

In summer the solar-driven and storm-induced circulations coincide during the major part of the day and moderately disturbed neutral composition with a decreased O/N_2 ratio is spread down to lower latitudes (Prölss, 1980; Prölss & von Zahn, 1977). Therefore, in summer one should expect a relatively small decrease in neutral gas density during the recovery storm phase even under severe magnetic storms. Our analysis of July 2004 storm period has shown a 5–7% decrease of neutral gas density not related to solar and geomagnetic activity variations.

4. Conclusions

The results of our analysis may be formulated as follows.

1. A daytime decrease of neutral gas density not related to solar and geomagnetic activity variations does take place at middle latitudes during the recovery storm phase in nonwinter seasons.
2. The effect is due to a storm-induced decrease of atomic oxygen concentration in the upper atmosphere. Contrary to the NO overcooling concept neutral temperature is not lower during the recovery storm phase compared to the prestorm reference day. But this depends on the level of geomagnetic activity.
3. Negative N_mF_2 deviations during the recovery storm phase related to low atomic oxygen concentration may serve as an indicator of a decreased neutral gas density.
4. In winter when according to F_2-layer storm morphology dominate positive N_mF_2 deviations or monthly median N_mF_2 take place at middle latitudes no decrease of neutral gas density is expected during the recovery storm phase.
5. There is no need to attract a new poststorm NO overcooling concept contradicting both empirical thermospheric models on Tex and neutral gas density observations during winter season. An explanation to the observed neutral density decrease during the recovery storm phase may be given in the framework of the well-known F_2-layer storm mechanism. This mechanism includes (a) auroral heating of the upper atmosphere, (b) changing of the thermospheric neutral composition due to upwelling in the auroral zone, and (c) the transfer of disturbed neutral composition with low atomic oxygen to middle latitudes by the thermospheric wind resulted from the interaction of solar-driven and storm-induced circulations. This mechanism is known to explain F_2-layer storm morphology and it is sufficient to explain neutral gas density variations during the recovery storm phase as in both cases the disturbed thermospheric circulation and variations of atomic oxygen are the controlling processes.

Acknowledgments
The Juliusruh data are kindly provided by Leibniz institute of Atmospheric Physics - Field station Juliusruh, Germany (http://www.sws.bom.gov.au/World_Data_Centre/1/3). The Rome data are provided by Istituto Nazionale di Geofisica e Vulcanologia (http://www. eswua.ingv.it/). The authors thank the Lowell DIDBase through GIRO to provide ionospheric data (http://giro.uml.edu/). The authors thank the European Space Agency to provide Swarm data (https://earth.esa.int/web/guest/swarm/data-access) and GFZ German Research Center for CHAMP data (ftp://anonymous@isdcftp.gfz-potsdam.de/champ/).

References

Bates, D. R. (1959). Some problems concerning the terrestrial atmosphere above the 100 km level. *Proceedings of the Royal Society A*, *253*, 451–462. https://doi.org/10.1098/rspa.1959.0207

Caruana, J. (1990). Solar-Terrestrial Prediction: Proc. Workshop at Leura, Australia, October 16–20, 1989, 257–263.

Chen, X., & Lei, J. (2018). A numerical study of the thermospheric overcooling during the recovery phases of the October 2003 storms. *Journal of Geophysical Research: Space Physics*, *123*, 5704–5716. https://doi.org/10.1029/2017JA025120

Duff, J. W., Dothe, H., & Sharma, R. D. (2003). On the rate coefficient of the $N(2D) + O_2 \rightarrow NO + O$ reaction in the terrestrial thermosphere. *Geophysical Research Letters*, *30*(5), 1259. https://doi.org/10.1029/2002GL016720

Duncan, R. A. (1969). *F*-region seasonal and magnetic storm behavior. *Journal of Atmospheric and Terrestrial Physics*, *31*, 59–70. https://doi.org/10.1016/0021-9169(69)90081-6

Field, P. R., Rishbeth, H., Moffett, R. J., Idenden, D. W., Fuller-Rowell, T. J., Millward, G. H., & Aylward, A. D. (1998). Modelling composition changes in *F*-layer storms. *Journal of Atmospheric and Solar - Terrestrial Physics*, *60*, 523–543. https://doi.org/10.1016/s1364-6826(97)00074-6

Forbes, J. M., Gonzalez, R., Marcos, F. A., Revelle, D., & Parish, H. (1996). Magnetic storm response of lower thermospheric density. *Journal of Geophysical Research*, *101*, 2313–2319. https://doi.org/10.1029/95ja02721

Fuller-Rowell, T. J., Codrescu, M. V., Moffett, R. J., & Quegan, S. (1994). Response of the thermosphere and ionosphere to geomagnetic storm. *Journal of Geophysical Research*, *99*, 3893–3914. https://doi.org/10.1029/93ja02015

Ivanov-Kholodny, G. S., & Mikhailov, A. V. (1986). *The prediction of ionospheric conditions*. Dordrecht: Reidel.

Lei, J., Burns, A. G., Thayer, J. P., Wang, W., Mlynczak, M. G., Hunt, L. A., et al. (2012). Overcooling in the upper thermosphere during the recovery phase of the 2003 October storms. *Journal of Geophysical Research*, *117*, A03314. https://doi.org/10.1029/2011JA016994

Mikhailov, A. V., Depueva, A. K., & Depuev, V. K. (2007). Daytime F_2-layer negative storm effect: What is the difference between storm-induced and *Q*-disturbance events? *Annales Geophysicae*, *25*, 1531–1541. https://doi.org/10.5194/angeo-25-1531-2007

Mikhailov, A. V., Depueva, A. K., & Leschinskaya, T. Y. (2004). Morphology of quiet time F_2-layer disturbances: High and lower latitudes. *International Journal of Geomagnetism and Aeronomy*, *5*, GI1006. https://doi.org/10.1029/2003GI000058

Mikhailov, A. V., & Perrone, L. (2019). Longitudinal variations in thermospheric parameters under summer noontime conditions inferred from ionospheric observations: A comparison with empirical models. *Scientific Reports*, *9*, 12763. https://doi.org/10.1038/s41598-019

Mikhailov, A. V., Perrone, L., & Smirnova, N. V. (2012). Two types of positive disturbances in the daytime mid-latitude F_2-layer: Morphology and formation mechanisms. *Journal of Atmospheric and Solar - Terrestrial Physics*, *81-82*, 59–75. https://doi.org/10.1016/j.jastp.2012.04.003

Mikhailov, A. V., Skoblin, M. G., & Förster, M. (1995). Day-time F_2-layer positive storm effect at middle and lower latitudes. *Annales Geophysicae*, *13*, 532–540. https://doi.org/10.1007/s00585-995-0532-y

Perrone, L., & Mikhailov, A. V. (2018). A new method to retrieve thermospheric parameters from daytime bottom-side Ne(h) observations. *Journal of Geophysical Research: Space Physics*, *123*, 10,200–10,212. https://doi.org/10.1029/2018JA025762

Picone, J. M., Hedin, A. E., Drob, D. P., & Aikin, A. C. (2002). NRLMSISE-00 empirical model of the atmosphere: Statistical comparison and scientific issues. *Journal of Geophysical Research*, *107*, 1468. https://doi.org/10.1029/2002JA009430

Prölss, G. W. (1980). Magnetic storm associated perturbations of the upper atmosphere: Recent results obtained by satellite-borne gas analyzers. *Reviews of Geophysics and Space Physics*, *18*, 183–202. https://doi.org/10.1029/rg018i001p00183

Prölss, G. W. (1995). Ionospheric F-region storms. In H. Volland (Ed.), *Handbook of Atmospheric Electrodynamics* (Vol. 2, pp. 195–248). Boca Raton: CRC Press.

Prölss, G. W., & von Zahn, U. (1977). Seasonal variations in the latitudinal structure of atmospheric disturbances. *Journal of Geophysical Research*, *82*, 5629–5632. https://doi.org/10.1029/ja082i035p05629

Reinisch, B. W., Galkin, I. A., Khmyrov, G., Kozlov, A., & Kitrosser, D. F. (2004). Automated collection and dissemination of ionospheric data from the digisonde network. *Advances in Radio Science*, *2*, 241–247. https://doi.org/10.5194/ars-2-241-2004

Rishbeth, H. (1998). How the thermospheric circulation affects the ionospheric F_2-layer. *Journal of Atmospheric and Solar - Terrestrial Physics*, *60*, 1385–1402. https://doi.org/10.1016/s1364-6826(98)00062-5

Rishbeth, H., Fuller-Rowell, T. J., & Rodger, A. S. (1987). *F*-layer storms and thermospheric composition. *Physica Scripta*, *36*, 327–336. https://doi.org/10.1088/0031-8949/36/2/024

Rishbeth, H., & Muller-Wodarg, I. C. F. (1999). Vertical circulation and thermospheric composition: A modelling study. *Annales de Geophysique*, *17*, 794–805. https://doi.org/10.1007/s00585-999-0794-x

Skoblin, M. G., & Förster, M. (1993). An alternative explanation of ionization depletions in the winter night-time storm perturbed F_2-layer. *Annales Geophysicae*, *11*, 1026–1032. https://doi.org/10.1007/s00585-995-0277-7

Turner, J.F., (1968). *The development of the ionospheric index T, IPS Series R Report, R11, June*. Australia: Ionospheric prediction service.

Woods, T. N., Eparvier, F. G., Harder, J., & Snow, M. (2018). Decoupling solar variability and instrument trends using the Multiple Same-Irradiance-Level (MuSIL) analysis technique. *Solar Physics* (2018), *293*, 76. https://doi.org/10.1007/s11207-018-1294-5

Zhang, Y., Paxton, L. J., Lu, G., & Yee, S. (2019). Impact of nitric oxide, solar EUV and particle precipitation on thermospheric density decrease. *Atmospheric and Solar-Terrestrial Phys.*, *182*, 147–154. https://doi.org/10.1016/j.jastp.2018.11.016